

## Theory of radiative shocks in optically thick media

R. P. Drake

*Atmospheric Oceanic and Space Sciences, Space Physics Research Laboratory, University of Michigan, Ann Arbor, Michigan 48109*

(Received 6 June 2006; accepted 22 February 2007; published online 5 April 2007)

The theory of radiative shocks in optically thick media is discussed, using exact relations for the fluid dynamics quantities. A quantitative, semianalytic approach to the radiation transport is presented here, based on the observation that the mean intensity is essentially constant through the cooling layer. This permits a self-consistent three-layer solution, in which the temperature upstream of the density jump never strictly equals the final downstream temperature. The development of the diffusive structure in the precursor is not fundamentally tied to the downstream properties. Portions of the precursor may be transmissive or diffusive. © 2007 American Institute of Physics.

[DOI: [10.1063/1.2716639](https://doi.org/10.1063/1.2716639)]

### I. INTRODUCTION

Radiative shocks are shock waves that are so strong that the radiative energy flux and/or pressure plays an essential role in the dynamics. Radiative shocks occur in many astrophysical systems, where they move into an *upstream* medium, leaving behind them an altered *downstream* medium. The structure includes a radiative precursor, a density jump, a cooling layer, and a final state (see Fig. 1). Key parameters include the shock velocity, the upstream density, and the upstream and the downstream *optical depth*, which designates the spectrally weighted mean, for the thermally induced radiation, of the number of exponential absorption depths through a region. When its optical depth is large, a region is said to be *optically thick*. The various regimes of radiative shocks are determined by the upstream and downstream optical depth, and are discussed in Drake<sup>1</sup> (p. 296ff). The present paper is concerned with radiative shocks in media that are optically thick both upstream and downstream, designated here as OTR (optically thick radiative) shocks. It introduces an approach to self-consistent calculation of the shock structure based on the observation that the mean radiation intensity is nearly constant downstream of the density jump. The results suggest some refinement of the established view that there is a “critical shock” and a “supercritical regime” for such shocks, in which the upstream temperature at the shock strictly equals the final downstream temperature.

OTR shocks have similarities and differences to ordinary hydrodynamic shocks. Upstream of all steady shocks there is a steady incoming flow of matter. This provides the energy flux that enables all the subsequent dynamics. Downstream of all steady shocks there is a steady outflow of matter and either zero or steady net radiation flux. Radiative shocks are distinct because of the large differences in key spatial scales. The radiation is emitted and absorbed over the largest scale, creating a precursor region upstream of the density jump and a cooling region downstream of it. The smallest scale is the viscous scale, on which the density jump occurs. Any shock heats particles in proportion to their mass, so the ion heating by the shock is much larger than the direct heating of the electrons. As a result, there is also a spatial scale downstream

of the density jump, on which the electron and ion temperatures equilibrate.<sup>2</sup> This scale can be much smaller than the radiative scales, as is discussed in pp. 331–333 of Drake<sup>1</sup> and pp. 515–522 of Zel’dovich and Razier,<sup>3</sup> and so we ignore electron-ion equilibration here. Electron heat conduction can also introduce a spatial scale. This can become significant when a radiating shock is driven outward from a hot, low-density source,<sup>4</sup> but more typically can be ignored as we do here.

Figure 1 shows the schematic structure of an OTR shock. There is zero radiation flux in the distant and undisturbed upstream region of density, temperature, and pressure  $\rho_o$ ,  $T_o$ , and  $p_o$ , respectively. As one moves toward the shock, the first change of these parameters occurs in a region where local emission from the precursor is not important, and where the temperature increases exponentially with distance because of heating by the decaying radiation flux. This is labeled the *transmissive precursor* in the figure. Under the conditions described below, the precursor also includes the region labeled the *diffusive precursor* in the figure, which can be much larger. This region is similar to a Marshak radiation wave, discussed in pp. 287–291 of Drake<sup>1</sup> and pp. 552–557 of Mihalas and Weibel-Mihalas,<sup>5</sup> in which radiation from a constant-temperature source penetrates and heats a medium. A sharp jump in density and temperature occurs at the location required to achieve the required balance of mass, momentum, and energy fluxes. This jump occurs on a spatial scale of a few ion-ion mean-free-paths. Beyond it, the shock-heated matter cools by emitting radiative energy from a *cooling layer*, in both directions. This cooling layer turns out to be optically thin, and to be extremely thin for very strong shocks. The cooling layer extends from the density jump downstream to a point where the net radiation flux reaches small values and the density and temperature are near their final values. On both sides of the cooling layer there is an adaptation zone several optical depths in extent where the radiation isotropizes and where the radiation flux, density, and temperature gradually cease to be influenced by the cooling layer. We discuss this structure and the reasons it exists in the following.

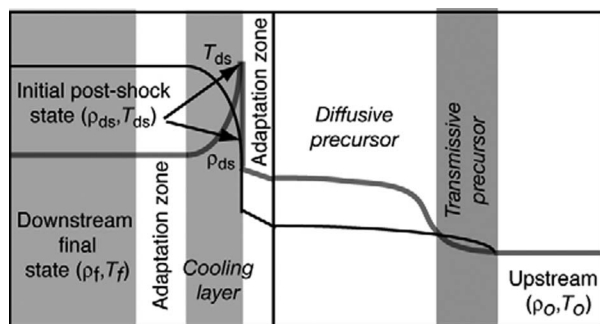


FIG. 1. Schematic of OTR shock moving from left to right, not to scale. The black curve is density and the thick curve is temperature. The shock transition includes a precursor region, upstream of the density jump, which has a transmissive section and may have a diffusive section (see later discussion). The shocked matter cools by radiating energy from the cooling layer into the other regions. The cooling layer is in all cases optically thin, while the precursor is optically very thick and is in fact enormous in scale by comparison. There are two adaptation zones across which the influence of radiation from the cooling layer fades.

Astrophysical examples of OTR shocks include some shocks in accretion disks,<sup>6</sup> shocks produced when active galactic nuclei capture stars,<sup>7</sup> and shocks within stars.<sup>8</sup> In particular, shocks form within the atmospheres of pulsating variable stars<sup>9</sup> such as Cepheid variables, RR Lyrae, W Virginis, RV Tau, and Mira-type<sup>10</sup> stars, and can be observed when they emerge from them. An improved conceptual understanding and ability to simply model the primary features of such shocks may lead to a better interpretation of such data.

Laboratory experiments are beginning to study radiative shocks,<sup>2,11–18</sup> and may have produced OTR shocks in converging geometries.<sup>19,20</sup> One example of such experiments is those reported<sup>18</sup> by Reighard *et al.* In this case a planar slab of Be is shocked and accelerated by laser irradiation to a velocity above 100 km/s. The slab then acts as a piston, driving a strongly radiative shock through xenon gas of an initial density of 6 mg/cm<sup>3</sup>. Having established that strongly radiative shocks can be produced and diagnosed, the next question for such experiments is what further work will be of greatest value. This leads one to ask what are the physical regimes that may be most challenging for computer simulations, and whether one can design benchmark experiments focused on such regimes. Likewise, while the existing experiments are not OTR shocks, as they are optically thin upstream, improved simple models enhance one's ability to design such experiments and assess their feasibility and scalings. OTR shocks are in any event a challenging problem for numerical simulations, given the vast disparities in the important scales along with the challenges of radiative transfer. The performance of such simulation codes ought to be measured in part by comparison to the simple and exact relations for the fluid dynamics given below.

The existing theoretical literature for OTR shocks is inadequate, by modern standards, in certain respects. The fluid dynamics, which provides the fundamental requirements of conservation of mass, momentum, and energy, is too often treated approximately.<sup>21,22</sup> The radiation transport has at times been treated with an equilibrium diffusion, near local-thermodynamic-equilibrium (near-LTE) model,<sup>23</sup> although

we see below that such a model does not apply in parts of the shock structure. The classic book by Zel'dovich and Raizer<sup>3</sup> employs an approximate analysis on pp. 526–543 and concludes that there is a critical velocity for such OTR shocks, corresponding to equality between the upstream and downstream material temperatures, and that this critical velocity divides the shock structure into *subcritical* and *supercritical* regimes. This conclusion is extensively if subtly qualified in Zel'dovich and Raizer. If one closely reads their discussion, it becomes clear that the work done is approximate and is in fact insufficient to precisely characterize the nature of the transition between regimes or the properties of the supercritical regime. (With regard to the fluid dynamics, their Eq. 7.50 in Sec. VII.16 is approximate.) Among its other functions, the present work provides a more detailed examination of these issues.

Unfortunately, however, much of the work in this area subsequent to Zel'dovich and Raizer is less carefully qualified. On pp. 557–573, Mihalas and Weibel-Mihalas<sup>5</sup> employ an analysis labeled as “semiquantitative,” but nonetheless give the impression that there is a distinct regime when the shock velocity exceeds a critical value that can be described as a supercritical regime. This conclusion is picked up<sup>21</sup> without qualification by Sincell *et al.*, who state “if the shock wave is strong enough, radiation from the shocked gas heats the material upstream from the shock until  $T_-$  (the upstream temperature) equals  $T_+$  (the final temperature) and the shock becomes supercritical” (definitions added). Some further remarks on this particular paper can be found in the Appendix. Turner and Stone<sup>22</sup> in turn pick up the same stark conclusion from the previous work. As experiments are emerging that begin to approach such conditions, one continues to see the stark and ultimately false description of the transition in the behavior of radiative shock waves appear in talks and in papers.

Though not specific to the present discussion, two other discussions of radiative shocks are worth mentioning. First, the recent book by Castor<sup>24</sup> offers an alternative semiquantitative analysis on p. 322 but does not explicitly address the meaning of the supercritical regime. Second, a paper<sup>25</sup> by Winkler *et al.* shows simulation results, free of the problems discussed in the Appendix, of a very strong radiative shock in a system that is optically thin upstream of the shock. Here, we present a quantitative semianalytic analysis that leads to a straightforward, easily calculated model of both the post-shock region and the cooling layer. We conclude from the pursuit of this model that the so-called supercritical regime is better viewed as a limiting case for very strong shocks.

In the analysis of OTR shocks, as seen in pp. 526–543 of Zel'dovich and Raizer<sup>3</sup> and pp. 557–573 of Mihalas and Weibel-Mihalas,<sup>5</sup> the regime of primary interest is the “flux-dominated regime,” in which the radiative energy fluxes exceed the material energy fluxes but the radiation pressure remains negligible. Present-day experiments are in this regime. The contrasting regime, in which the radiation pressure exceeds the material pressure, is much simpler because the radiation, entrained in the matter, behaves like an ideal gas having a polytropic index,  $\gamma$ , equal to 4/3. This regime requires higher-temperatures and so is less common in astro-

physics and remains more distant in the laboratory. It does exist, for example, in the blast waves of core-collapse supernovae.<sup>26</sup> In the remainder of this paper we consider only steady, planar, OTR shocks in the flux-dominated regime, treated in a frame of reference in which the shock is at rest (the “shock frame”) and in which the flow is normal to the shock. Thus, our problem here is distinct from that of the large literature (see, for example, Ref. 9) treating the complications involved in line-emission-dominated, optically thin, radiative shocks.

## II. FLUID-DYNAMIC THEORY

We proceed now with a specific theory. Our goal is to develop the simplest possible model that captures the essential behavior of these shocks. Our approach will be to construct a three-layer model, consisting of the final state, the cooling layer, and the precursor. This allows us to work with fairly simple radiative transfer calculations, as we will see. However, such a model cannot capture the precise effects of the two adaptation zones. These will be discussed qualitatively. Note that our goal is not to develop an exact solution of the radiative transfer aspects of this problem, which is numerically much more complex.

To proceed, we designate the electron and ion temperatures by  $T$ , assuming a polytropic gas with index  $\gamma$ , and an incoming upstream flow at speed  $-u_s$  with (for simplicity) zero pressure. (We use the minus sign before  $u_s$  taking positive radiation flux to the right and the incoming flow moving to the left, and write the “shock speed”  $u_s$  as a positive number.) Several features of the shock structure are set by fluid dynamics, and are independent of any details of radiation transport. The continuity and momentum equations provide two conditions on the flow,

$$\rho u = -\rho_o u_s, \tag{1}$$

and

$$\rho u^2 + p = -(\rho_o u_s)u + p = \rho_o u_s^2, \tag{2}$$

in which the mass density is  $\rho$ , the flow velocity is  $u$ , the pressure is  $p$ , and we designate any arbitrary point in the flow with no index, using indices  $o$  for the initial state,  $f$  for the final state,  $ds$  for downstream at the density jump,  $us$  for upstream at the density jump, and otherwise as appropriate. We define the normalized pressure as  $p_n = p/(\rho_o u_s^2)$  and the normalized specific pressure (proportional to specific thermal energy) as  $RT_n = RT/u_s^2$ , where  $R$  is the “gas constant” (here assumed to be constant for simplicity) so  $p = \rho RT$ . Defining the inverse compression,  $\eta = \rho_o/\rho$ , Eqs. (1) and (2) imply that

$$p_n = (1 - \eta) \tag{3}$$

and

$$RT_n = \eta(1 - \eta). \tag{4}$$

These two equations reflect the fact that the highest pressure obtainable in compressible fluid flow corresponds to the lowest velocity and thus the highest density. To create a change in the pressure energy must flow to cause the temperature to have the value demanded by conservation of mass and mo-

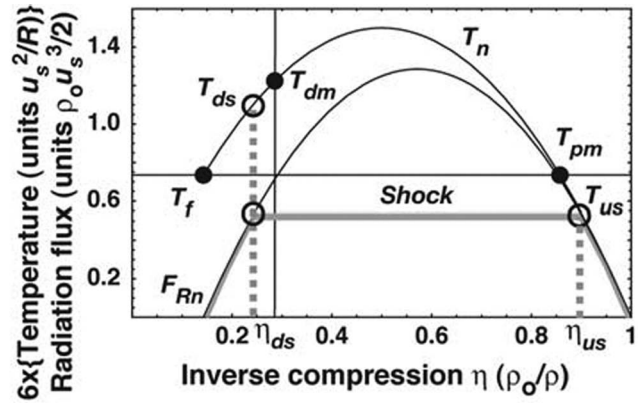


FIG. 2. Fluid dynamics implications. The normalized radiation flux must follow the lower curve or jump in  $\eta$  while maintaining constant  $F_{Rn}$ . The temperature is determined solely by the value of  $\eta$ . The open circles show one possible case. The final temperature is always  $T_f$ . The limiting temperatures (postshock  $T_{dm}$  and precursor  $T_{pm}$ ) are labeled with solid dots.

mentum. The energy equation, with the internal energy density taken to equal  $p/(\gamma-1)$  and the radiation flux designated by  $F_R$ , provides a further condition on the flow, which is

$$F_R + \frac{\gamma}{\gamma-1} p u + \frac{\rho u^3}{2} = -\frac{\rho_o u_s^3}{2}. \tag{5}$$

This equation makes evident a notable feature of radiative shocks, that any increase in the (rightward) radiation flux is balanced by an increase in the (leftward) flow of material energy. After introducing the normalized radiation flux as  $F_{Rn} = 2F_R/(\rho_o u_s^3)$ , which physically represents the ratio of the radiation flux to the kinetic energy flux coming in from upstream, Eqs. (3)–(5) imply

$$F_{Rn} = -1 + \frac{2\gamma}{\gamma-1} \eta - \frac{\gamma+1}{\gamma-1} \eta^2. \tag{6}$$

The above equations are exact solutions. Thus, as a consequence only of the simple fluid dynamics, the pressure, temperature, and radiation flux change in defined ways as the density changes. The implications of the above relations are often shown in a plot like that of Fig. 2 (with numbers for  $\gamma=4/3$ , corresponding approximately to an ionizing medium as discussed in pp. 66–90 of Drake<sup>1</sup>). The density, temperature, and radiation flux all increase in the precursor region until reaching the density jump, where the temperature is  $T_{us}$ . The transition in density is controlled by the physical requirement that the radiation flux be constant across the density transition (following the solid gray line in the figure), with the implications that the postdensity-jump temperature  $T_{ds}$  (at the top of the dashed gray line) exceeds the predensity-jump temperature and that the final temperature  $T_f$  is reached when the radiation flux has declined to zero (for an OTR shock). Here we consider only shocks with a discontinuous jump in density, leaving the regimes of continuous transitions to other work.<sup>5,27</sup>

In the final state,  $\eta_f = (\gamma-1)/(\gamma+1)$  and  $RT_{nf} = 2(\gamma-1)/(\gamma+1)^2$ . Figure 2 seems to suggest that  $T_{us}$  might equal or exceed the final temperature,  $T_f$ . One can approximately exclude the case  $T_{us} > T_f$  on thermodynamic grounds (see p.

530 of Zel'dovich and Razier<sup>3</sup>). If  $T_{us}=T_f$ , then the maximum temperature  $T_{ds}$  is given by  $RT_{ndm}=(3-\gamma)RT_{nf}$ . The adaptation zones complicate this picture without creating large changes. In the upstream adaptation zone, the influence of radiation from the cooling layer causes a slight increase in temperature immediately upstream of the density jump. Thus,  $T_{us}$ ,  $T_{pm}$ ,  $T_{ds}$ , and  $T_{dm}$  will all be slightly larger in reality than we will find using the three-layer model developed here. In the downstream adaptation zone,  $T$  will approach  $T_f$  more slowly than the three-layer model will predict.

Development of the three-layer model proceeds as follows. One can quantify the relation between  $T_{us}$  and  $T_f$  by setting  $T_{us}=f_s T_f$  and finding the values of  $\eta$  at the density jump corresponding to this temperature. It is helpful to define a shock strength parameter  $Q$  as  $2\sigma u_s^5/(R^4 \rho_o)$ . This implies that  $\sigma T_f^4/(\rho_o u_s^3/2)=16 Q(\gamma-1)^4/(\gamma+1)^8$ . For reference, an experiment<sup>18</sup> that drives a shock at 100 km/s through Xe gas ionized 15 times has  $Q\sim 10^5$ . One can then use Eqs. (3)–(6) to find  $\eta_{ds}$  and  $\eta_{us}$  (and thus  $\rho_s$ ,  $\rho_{us}$ ,  $T_{ds}$ ,  $T_{us}$ , and  $F_R$ ). Finding the spatial profile of  $\eta$  is thus sufficient to describe the shock structure. One finds an equation for this profile by taking the spatial derivative in  $z$  of Eq. (6), which gives

$$-\frac{\partial F_{Rn}}{\partial z} = \left[ \frac{-2\gamma + 2\eta(\gamma+1)}{\gamma-1} \right] \frac{\partial \eta}{\partial z}, \quad (7)$$

which one can alternatively obtain from the traditional “gas-energy” equation for the internal energy of the gas. In order to close the set of equations, one needs one or more additional equations describing the behavior of the radiation. We discuss this next.

### III. POSSIBLE RADIATION TRANSPORT MODELS

We now turn to the specification of the radiation transport, which will permit us to find the profile of an OTR shock. To find the profile one must determine  $\partial F_R/\partial z$ , which represents radiative cooling or heating, as a function of known or calculated parameters. One could use an equilibrium diffusion model, in which  $F_R \propto \partial T/\partial z \propto \partial \eta/\partial z$ , to obtain a second-order differential equation for  $\eta$ , but this would preclude the correct treatment of the two nonequilibrium regions discussed below and is a very poor choice.

Two other choices both involve the use of the radiative transfer equation written here as

$$\frac{1}{c} \frac{\partial I_R}{\partial t} + \frac{\partial I_R}{\partial s} = \int \kappa_\nu (B_\nu - I_\nu) d\nu + \int \sigma_\nu (J_\nu - I_\nu) d\nu, \quad (8)$$

in which the radiation intensity (energy flux per sr) is  $I_R$ , the path of the radiation is described by  $s$ ,  $c$  is the speed of light, and the integrals are over all frequencies  $\nu$ . Within the integrals, the subscript  $\nu$  indicates spectral dependence with units as appropriate. The functions involved are the absorption opacity  $\kappa_\nu$ , the scattering opacity  $\sigma_\nu$ , the spectral thermal intensity (the Planck function)  $B_\nu$ , the spectral radiation intensity  $I_\nu$ , and the mean of the spectral intensity over all solid angles,  $J_\nu$ . This equation is written in the geometric-optics limit, which is relevant to radiative shocks, and under

the assumption that the scattering is elastic and isotropic. It can be viewed fundamentally as a kinetic equation for the photons. We will ignore the time-dependent term because the radiation reaches steady state instantaneously on the time scales of material motion.

Assuming only isotropic, elastic scattering and steady state, the zeroth moment over angle of the radiative transfer equation gives

$$\partial F_R/\partial z = 4\pi\kappa_p(B - J_R) \quad (9)$$

in one dimension, in which the thermal intensity is  $B = \sigma T^4/\pi$ ,  $J_R$  is the mean radiation intensity averaged over all solid angles,  $J_R = \int_{4\pi} I_R d\Omega/(4\pi)$ , with radiation intensity (energy flux per sr)  $I_R$ , and Planck mean opacity  $\kappa_p$ , with units of inverse length and assumed as usual to be accurate for  $J_R$  in addition to  $B$ . If one makes the further assumption of radiation isotropy, this equation describes the radiation-matter energy exchange in the typical nonequilibrium-diffusion models discussed in books.

Equations (1)–(9), however, are still not sufficient to solve for the structure of the system, because Eq. (9) introduces the new variable  $J_R$ . So one needs some additional constraint on  $J_R$ . A very common approach to this is to use a diffusion model based on the steady-state, nonrelativistic first moment in photon direction of the radiation transfer equation for isotropic emission,

$$\frac{\partial p_R}{\partial z} = -\frac{\bar{\chi}}{c} F_R, \quad (10)$$

in which  $\bar{\chi}$  is an averaged opacity typically approximated as the Rosseland mean opacity,  $c$  is the speed of light, and  $p_R$  is the scalar radiation pressure. To avoid introducing yet another variable and requiring yet another equation for closure, one must work in the Eddington diffusion approximation, writing  $p_R = f_E E_R = f_E (4\pi/c) J_R$ , in which  $E_R$  is the radiation energy density. Equation (10) then becomes

$$4\pi f_E \frac{\partial J_R}{\partial z} = -\bar{\chi} F_R. \quad (11)$$

Here the Eddington factor  $f_E$ , assumed constant, accounts for the angular distribution of the radiation, and is 1/3 for an isotropic distribution and 1 for a beam-like one. Equation (11), combined with Eq. (9), closes the system of equations. This provides a sensible approach to finding the structure of any region that is many optical depths in extent. It is used below to find the structure of the radiative precursor. However, Eq. (11) is only accurate if  $f_E$  is sufficiently constant in space, which typically corresponds to gradient scale lengths of the parameters that are large compared to  $\bar{\chi}^{-1}$ , and if the gradients of  $p_R$  and  $J_R$  are parallel. Equation (11) proves to be qualitatively incorrect for the cooling layer in a radiative shock, as we will see in the next section. One cannot obtain an accurate solution for the behavior of the cooling layer, for strong radiative shocks, using this type of diffusive model of the radiation transport. (See Sec. IV for some discussion of more complete radiative transfer solutions.)

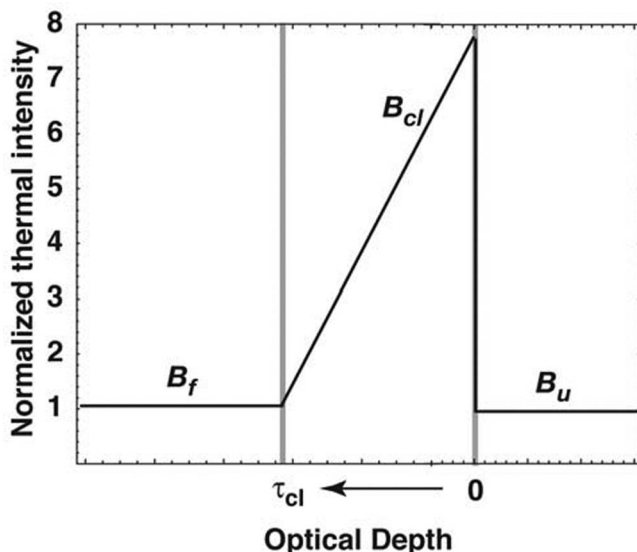


FIG. 3. Structure of the three layer model used to assess radiation properties.

Here we introduce an alternative and more accurate closure of the relevant equations for the downstream region, by making the key observation, that for strong OTR shocks  $J_R$  changes negligibly as one traverses the optically thin cooling layer. This is apparently a new observation. This statement becomes more accurate as the shock strength increases, as is also shown in the next section. This is because (a) the flux emitted from an optically thin sublayer is equal in both directions, so that  $J_R$  would be identically constant if the angular distribution of the radiation did not change, and (b) the changes to the angular distribution in the cooling layer are localized to a very small range of angles and have a small effect on  $J_R$ .

Before we turn to the completion of the calculation, it is worthwhile to discuss the previous two paragraphs in more depth and in a quantitative way. The idea that a nonequilibrium diffusion model [using Eq. (10)] is generally a valid one that provides a tractable approach to problems such as this is very entrenched in the community concerned with radiation hydrodynamics. For the case of strong radiative shocks in the flux-dominated regime, this turns out to not be the case. We show this using both qualitative arguments and a quantitative, simple three-layer model in the next section.

#### IV. RADIATIVE TRANSFER IN A SIMPLE MODEL

One can learn much about the qualitative behavior of radiation in OTR shocks using the simple three-layer model illustrated in Fig. 3. The first region in such a model is the downstream region, assumed to be optically very thick and to have temperature  $T_f$  and the thermal intensity  $B_f$ . The second region is the cooling layer, treated here as a zone of unknown effective optical depth  $\tau_{cl}$ , which is the optical depth necessary to achieve energy balance as shown below. The temperature is  $T_{ds}$  at the upstream edge of this zone and is  $T_f$  at the downstream edge. The thermal intensity within the cooling layer,  $B_{cl}(\tau)$ , is assumed to decrease linearly with

optical depth  $\tau$  from the upstream edge to the downstream edge. This is of course an approximation; the actual profile does decrease monotonically but not with this shape. In the actual system the transition between the cooling layer and the downstream layer will also be continuous, not abrupt. The third region in such a model is the precursor region, assumed to be optically very thick, having a temperature  $T_{us}=f_s T_f$ , and assumed to have an emissivity (the ratio of the radiance emitted toward downstream to  $\sigma_B T_{us}^4$ , where  $\sigma_B$  is the Stefan-Boltzmann constant) of approximately unity. This will be shown elsewhere to be quantitatively correct for strong OTR shocks. The calculations that follow make extensive use of the steady solution of the planar radiative transfer equation, here represented as

$$I_R(\tau_2) = I_R(\tau_1) e^{-(\tau_2 - \tau_1)/\mu} + \int_{\tau_1}^{\tau_2} B(\tau) \frac{e^{-(\tau - \tau_1)/\mu}}{\mu} d\tau, \quad (12)$$

which relates the intensity at the optical depth (along the  $z$  axis)  $\tau_2$  to the intensity at  $\tau_1$  and the emission and attenuation between  $\tau_1$  and  $\tau_2$ , with  $\tau$  defined so  $\tau_2 > \tau_1$ . The angular variable that accounts for variations in direction is  $\mu = \cos \theta$ , where  $\theta$  is the angle to the  $+z$  axis. Working with Eq. (12) one is able to take the appropriate moments in the angle to find the radiation properties.

We will first use the energy balance to find the effective optical depth of the cooling layer,  $\tau_{cl}$ . First we focus on the downstream boundary of the cooling layer. At this boundary in this model the radiation flux reaches zero, as the final state by definition has zero radiation flux. We can write an energy-flux-balance equation that expresses this result as

$$\sigma T_f^4 - 1.2\tau_{cl}\sigma T_{ds}^4 - f_s^4 \sigma T_f^4 (1 - \tau_{cl}) = 0. \quad (13)$$

We assume the cooling layer to be optically thin (as is confirmed later), so the factor  $(1 - \tau_{cl})$  in Eq. (13) is the expansion to first order of  $\text{Exp}[-\tau_{cl}]$ . The flux from the cooling layer is  $1.2\tau_{cl}$  times the flux that would be produced by a thick layer at the temperature  $T_{ds}$ . (The factor of 1.2 results from the integral of the radiation transfer equation over angle to find the flux from an optically thin layer given the assumed emission profile and isotropic emission. For this specific model and for sensible values of  $T_{ds}/T_f$ , this coefficient is accurate to 10% for both upstream and downstream emission from the cooling layer.)

Next we focus on the downstream edge of the precursor, where the radiation fluxes must equal the radiation flux from Eq. (6), so

$$\sigma T_f^4 (1 - \tau_{cl}) + 1.2\tau_{cl}\sigma T_{ds}^4 - f_s^4 \sigma T_f^4 = \left( -1 + \frac{2\gamma}{\gamma-1} \eta - \frac{\gamma+1}{\gamma-1} \eta^2 \right) \frac{\rho_0 u_s^3}{2}. \quad (14)$$

The three-layer model, expressed precisely in Eqs. (13) and (14), is used to determine  $\tau_{cl}$  in the profile of Fig. 3 and to estimate  $f_s$ . This calculation strictly enforces the boundary condition at the downstream boundary of the cooling layer. The radiative transfer calculation described below is not intended to reproduce that boundary condition. Instead, as we shall see, it provides a quantitative indication of the behavior

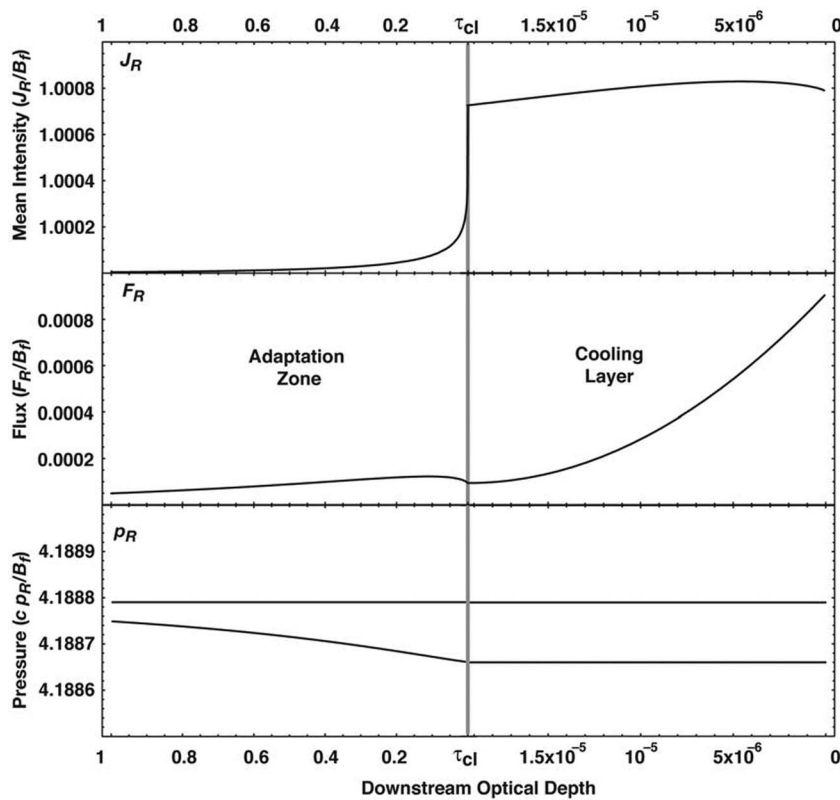


FIG. 4. Moments of the radiation intensity for the three layer model. The optical depth scale changes at the vertical gray line. In the plot of  $p_R$  the straight line represents the final downstream value.

of the downstream adaptation zone. Given that our goal is to assess the radiation properties in the strong OTR shock limit, we take limiting values, from the above fluid dynamics equations, as  $T_{ds} = (3 - \gamma)T_f$  and  $\eta_{ds} = 2(\gamma - 1)/(\gamma + 1)$ . Equations (13) and (14) can then be written as

$$1 - 1.2\tau_{cl}(3 - \gamma)^4 - f_s^4(1 - \tau_{cl}) = 0 \quad (15)$$

and

$$(1 - \tau_{cl}) + 1.2\tau_{cl}(3 - \gamma)^4 - f_s^4 = \frac{(3 - \gamma)(\gamma + 1)^7}{16Q(\gamma - 1)^4}. \quad (16)$$

For given values of  $Q$  and  $\gamma$  these two equations can be solved for  $\tau_{cl}$  and  $f_s$ . This gives a solution with self-consistent energy balance and the same approximate magnitudes and qualitative trends as the more-complete solution discussed in the next section. Specifically, with  $\gamma = 4/3$ , one finds  $f_s = 0.996$  and  $\tau_{cl} = 0.0019$  for  $Q = 10^5$  and  $f_s = 0.99996$  and  $\tau_{cl} = 0.000019$  for  $Q = 10^7$ . In general over the range of interest both  $\tau_{cl}$  and  $(1 - f_s)$  scale approximately as  $1/Q$ , justifying the assumption  $\tau_{cl} \ll 1$  used above.

This model provides a useful approach to evaluating the parameters for the radiation and the radiation transport. Specifically, we can use the radiative transfer equation to evaluate the spatial variation of the moments of the radiation intensity. This will produce results with correct qualitative trends. It is helpful to recall that for planar systems the radiation flux is the first moment of the radiation intensity in  $\mu$ ,  $F_R = 2\pi \int_{-1}^1 \mu I_R d\mu$ . The mean intensity  $J_R$  is the zeroth moment as defined above while the scalar radiation pressure is the second moment (divided by  $c$ ), so  $cp_R = 2\pi \int_{-1}^1 \mu^2 I_R d\mu$ . The radiation crossing the downstream cooling-layer boundary from further downstream in this model is isotropic, cor-

responding to the final, constant-temperature, optically thick, steady downstream region. The radiation crossing this boundary from upstream is not isotropic, but rather is slightly pancaked, because the more-oblique rays through the optically thin cooling layer will emerge with higher values of  $I_R$  than those nearer the axis of shock propagation. Because the flux corresponding to this radiation from upstream must balance the flux from the radiation from downstream, this implies that the on-axis value of  $I_R$  is slightly smaller from upstream than from downstream. Given the angular distribution of the radiation as just described, and given that the radiation flux is set fundamentally by the energy balance, the behavior of  $J_R$  and  $p_R$  will differ.  $J_R$  weighs all angles equally, while  $p_R$  more strongly weighs angles near the axis. As a result, and as we will see from direct calculation below, their gradients differ and in fact have an opposite sign in some regions.

Figure 4 shows the moments of  $I_R$ , downstream of the density jump, for a system corresponding to  $Q = 10^7$  and  $\gamma = 4/3$ . Here  $J_R$  is normalized to  $B_f$ ,  $F_R$  is normalized to  $B_f$ , and  $p_R$  is normalized to  $B_f/c$ . The ratio  $2B_f/\rho_0 u_s^3$  necessary to convert  $F_R$  as shown to the normalization of Eq. (6) and others above is  $(16/\pi)Q(\gamma - 1)^4/(\gamma + 1)^8$ . Here this is  $7.16Q/10^5$ . The only moment that changes strongly is the radiation flux, which decreases from a large value at the upstream boundary to a much smaller one at the cooling-layer boundary, and then adjusts and decreases slowly further downstream. The slight increase of  $F_R$  downstream of the cooling-layer boundary reflects the limitations of the three-layer model. It should be evident  $F_R$  must exponentially approach zero as one penetrates multiple optical depths into the downstream region. However, the value of  $F_R$  at the bound-

ary of the cooling layer and the adaptation zone found from the simple model (0.0001) corresponds from Eqs. (3)–(6) to a difference of 7% in temperature from the final state (as compared to the initial postdensity-jump difference of more than 65%). The temperature difference then decreases much more slowly toward the final value as the flux becomes negligible over a few optical depths. Correspondingly, we have designated this region the adaptation zone in Fig. 1. The physical quantities gradually change, although not by much, as they approach their final values. (In contrast, the simple model used to find the  $\tau_{cl}$  set  $F_R$  to zero at the cooling-layer boundary and ignored the adaptation zone.) A fully self-consistent solution would produce smoother curves but would not change the qualitative behavior.

The change in  $F_R$  through the cooling layer corresponds primarily to the change in the direction of the emission from downstream to upstream. Since  $J_R$  and  $p_R$  are both even functions of  $\mu$ , neither of them is sensitive to the upstream or downstream direction of the radiation flux and both these quantities have small gradients. The assumption suggested above that  $J_R = \text{constant}$  is accurate to 0.08% for this case. However,  $J_R$  is far more sensitive than  $p_R$  to the greatly increased intensity near  $\mu = 0$  in and near the cooling layer. In contrast  $p_R$  is more sensitive to the difference in temperature between the final state and the precursor ( $T_f - T_{us}$ ). The result is that through the adaptation zone and much of the cooling layer, the gradient of  $p_R$  opposes that of  $J_R$ . (The gradient of  $p_R$  remains negative in the cooling layer, even though the line appears flat in Fig. 4.) This has the implication that a simulation in the Eddington diffusion approximation cannot possibly obtain a correct calculation of the cooling-layer in a strong OTR shock. In particular, it will generate unphysical negative radiation fluxes in the cooling layer and the adaptation zone. One can produce a model of the downstream region using the nonequilibrium diffusion equations discussed below for the precursor. This has the effect of forcing the derivative of  $J_R$  to be negative throughout the profile, which is incorrect.

Because all the relevant quantities [ $1/B_f$ ,  $\tau_{cl}$ , and  $(1 - f_s)$ ] scale together as  $1/Q$ , the profiles of  $F_R$ ,  $J_R$ , and  $p_R$  have a very similar shape for all values of  $Q$  large enough that  $\tau_{cl} \ll 1$  and small enough that the system remains in the flux-dominated regime. As  $Q$  decreases, the relative change in  $J_R$  increases. For example, for  $Q \sim 10^5$  with  $\gamma = 4/3$   $J_R$  varies  $\sim 5\%$  through the cooling layer. Assuming  $J_R = \text{constant}$  still introduces only a small error in this case, as it is ( $J_R - B$ ) that matters and  $B$  increases more than sevenfold through the cooling layer. Here the value of  $F_R$  found from the simple model (0.01) again corresponds from Eqs. (3)–(6) to a difference of 7% in temperature from the final state (again as compared to the initial difference of more than 65%). The relative temperature difference is the same in the two cases because of the scaling of the normalization with  $Q$ . If one needed a more precise solution for the spatial profile of  $J_R$  and the downstream adaptation zone for this case, one could iterate the profile of  $J_R$  using the solution method discussed below.

## V. SOLUTIONS FOR THE PROFILES IN STRONG RADIATIVE SHOCKS

The realization that one can approximate  $J_R$  as constant through the cooling layer, and that this assumption becomes better as the shock gets stronger, greatly simplifies the calculation of the profiles. Because  $J_R$  is a continuous quantity, matching the cooling layer to the final state then requires  $J_R = B_f = \sigma T_f^4 / \pi$ . One can therefore express  $\partial F_R / \partial z$  as a function of  $\eta$  (and of the known quantities  $\gamma$  and  $Q$ ), so one can integrate Eq. (7) to find the cooling layer profile for any value of  $f_s$ . To do so, it is convenient to change variables from  $z$  to  $\tau$  using  $d\tau = -\kappa_P dz$ . Here for simplicity we assume constant and equal opacities; it would be a straightforward addition to parameterize their variation as functions of  $\eta$ . One can check the result by then integrating  $\partial F_R / \partial z$  using this profile and comparing  $F_R$  with the value from Eq. (6).

The model used here has points of similarity with those of Heaslet and Baldwin<sup>28</sup> and Farnsworth and Clarke.<sup>8</sup> It ignores the many complications that line transport of radiation may introduce, and so may be most directly applicable to dense laboratory plasmas and to conditions deep within dense stellar atmospheres.<sup>29</sup> Even so, these complications may also be viewed as subsumed within the definitions of the spectrally averaged opacities.

To find the structure in the precursor, one can use Eq. (11) for the evolution of  $J_R$ . We work with a normalized value of  $J_R$ ,  $J_{Rn} = J_R / (\rho_0 u_s^3 / 2)$ . The Eddington factor is taken here to be  $1/3$ , which corresponds to isotropic radiation. We discuss  $f_E$  in the precursor further below. Using this radiation flux in Eq. (6) and the transport model in Eq. (7), one obtains the following coupled differential equations for  $J_{Rn}$  and  $\eta$ ,

$$1 - \frac{2\gamma}{\gamma-1} \eta + \frac{\gamma+1}{\gamma-1} \eta^2 - f_E \frac{4\pi}{\bar{\chi}} \frac{\partial J_{Rn}}{\partial z} = 0 \quad (17)$$

and

$$2\pi\kappa_P \left[ J_{Rn} - \frac{Q}{\pi} (1 - \eta)^4 \eta^4 \right] = \left[ \frac{\eta(\gamma+1) - \gamma}{\gamma-1} \right] \frac{\partial \eta}{\partial z}. \quad (18)$$

One can integrate these equations from the leading edge of the precursor to the density jump, for any value of  $f_s$ . This is straightforward as the derivative of  $J_{Rn}$  with  $\eta$  turns out to be well defined as  $\eta$  approaches 1. To do so, one must parameterize in some way the opacities  $\kappa_p$  and  $\bar{\chi}$ . In the example given, for simplicity, we assume them to be equal and constant. Note that the Eddington factor effectively acts as a multiplier on  $\bar{\chi}$ , which scales the overall length of the precursor. It also contributes to the ratio  $f_E \kappa_P / \bar{\chi}$  which affects the relative size of the two regions in the precursor, discussed below.

To connect the solutions in the cooling layer and the precursor, and thus to determine  $f_s$  for a given  $Q$  and other parameters, one can use the fact that  $J_R = B_f$  at the density jump, because as above we have assumed that  $J_R$  has not changed across the cooling layer. At the density jump,  $J_R$  includes contributions from the precursor and from the downstream direction. The contribution from the precursor is half the value from the precursor calculation, as the assumption that the precursor radiation is effectively isotropic will

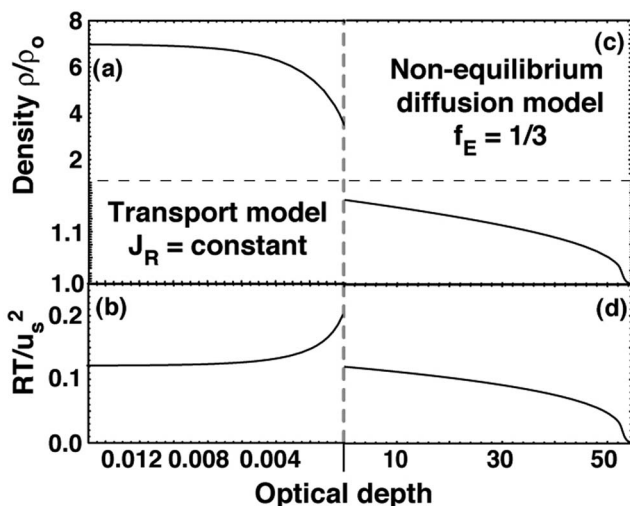


FIG. 5. Structure of an OTR shock for  $Q=10^5$ ,  $f_E=1/3$ , and  $\gamma=4/3$ . The density jump occurs at the vertical dashed line, where the optical depth scales change. The optical depth scale increases in both directions from the density jump. The panels show (a) cooling-layer density, (b) cooling layer temperature, (c) precursor density, and (d) precursor temperature. The density scale changes at the horizontal dashed line.

hold so long as the precursor is many optical depths in extent. The contribution from downstream,  $J_d$ , includes  $B_f/2$  from the final state plus the increase from the cooling layer, which we can determine by integrating in optical depth and angle through the cooling layer. The angular integral at any  $\tau$  introduces  $\Gamma(0, \tau)$ , the incomplete gamma function (or alternatively an exponential integral), giving

$$J_d = \frac{B_f}{2} + \frac{1}{2} \int_0^\infty (B(\tau) - B_f) \Gamma(0, \tau) d\tau, \quad (19)$$

in which  $B(\tau)$  is the thermal intensity. Only one value of  $f_s$  yields the necessary total value of  $J_R$  at the density jump. Figure 5 shows typical profiles of temperature and density.

The implications of the present model for the behavior of the temperature ratio  $T_{us}/T_f$  are seen in Fig. 6, which shows the dependence of  $(1-f_s)$  on  $Q$  for  $\gamma=4/3$ ,  $f_E=1/3$ , and constant, equal opacities. One finds that  $f_s$  approaches 1 only asymptotically. The reason is that the net radiation flux across the density jump never becomes zero and is always

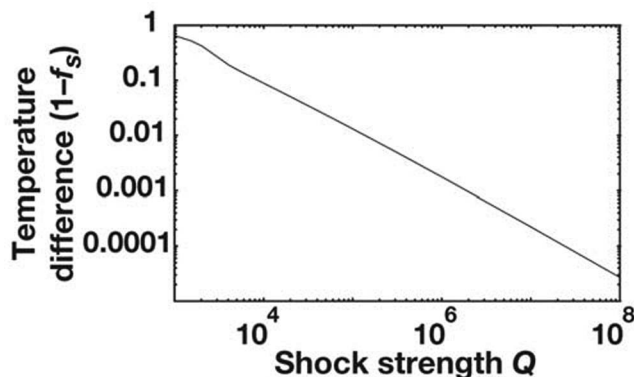


FIG. 6. Temperature ratio plotted as  $(1-f_s)=(1-T_{us}/T_f)$  vs the shock strength  $Q$  for  $f_E=1/3$ , and  $\gamma=4/3$ .

larger than the radiation flux produced by the cooling layer. One can distinguish between a quantity that can decay to zero, however slowly, and a quantity that can become arbitrarily small but that must remain nonzero by some definite amount. The latter case is what one has in these shocks.

### VI. DISCUSSION AND CONCLUSION

The solutions just described have some general features that merit discussion. For strong enough shocks, there is a *diffusive region* and a *transmissive region* in the precursor. Weaker shocks have only a transmissive region, but the development of the diffusive region occurs gradually as  $Q$  increases. For  $Q$  larger than a few thousand (for  $\gamma=4/3$ ), and near enough to the density jump, one can show from the fluid dynamics that  $F_R/c < 4\sigma T^4/c$ , so that the energy density in the radiation flux is less than the energy density of isotropic radiation corresponding to the local temperature. This represents the onset of a diffusive regime. As  $Q$  increases,  $F_R$  near the density jump becomes an ever-smaller fraction of  $4\sigma T^4$ . Moving upstream from the density jump, there is always some density in the precursor beyond which  $F_R/c > 4\sigma T^4/c$ . This boundary moves to smaller density as  $Q$  increases. In this region the radiation becomes beam-like within a few optical depths (radiation moving obliquely to the upstream direction is preferentially absorbed). One can show from Eqs. (17) and (18) that  $(1-\eta)$ ,  $F_R$ , and  $J_R$  thenceforth decrease exponentially as a function of  $\bar{\chi}z$ .

One can come away from the historical literature with a sense that finding  $T_{us} \sim T_f$  and a diffusive region in the precursor are causally connected developments. It is worth emphasizing, in contrast, that the appearance of the diffusive region is fundamentally a consequence of the fluid dynamics and not of the radiation transport. Furthermore, the presence of this region is connected with the energy density corresponding to the radiation flux and is not fundamentally related to achieving  $T_{us} \sim T_f$ . In the present model with  $\gamma=4/3$ , the diffusive region appears when  $f_s \sim 0.4$ . In a case with an incoming radiation flux from a downstream boundary, as might occur in a star, a diffusive region could appear in principle for a very large ratio of  $T_f$  to  $T_{us}$ , because the incoming radiation flux will hold  $T_f$  above the value it would have otherwise (see Fig. 2). In addition, the traditional description of the precursor structure does not extend to cases of an optically thin precursor (discussed on pp. 309–317 of Drake<sup>1</sup>), in which one tends to find  $T_{us} \sim T_f$  in all cases. These are additional reasons to be less than satisfied with the historical notion of a supercritical regime.

For simplicity the present model is a three-layer model, but this is also a limitation. The adaptation zones do alter the structure. We discussed above the downstream adaptation zone, through which the temperature and other parameters make their final, <10% adjustments as they seek their steady-state values. In the upstream region, through the adaptation zone in the precursor the angular distribution of  $I_R$  evolves to an isotropic shape. Small changes in the plasma parameters will also occur through this region. However, this zone extends only a few optical depths and the precursor is

tens to hundreds of optical depths in extent. As a result, we have chosen not to explore the precursor adaptation zone further here.

Another limitation of the model just described is in its assumption of constant  $f_E$  in the precursor. Variations in  $f_E$  effectively change the optical-depth scale as one traverses the precursor. In the transmissive regime  $f_E$  is 1, which will serve to lengthen this portion of the precursor. As the precursor enters the diffusive regime  $f_E$  transitions to  $1/3$ , then it drops below  $1/3$  very near the density jump, where the radiation from the cooling layer is pancaked. A next level of the semianalytic model development could account for this through either simple estimates or an iterative explicit calculation of  $f_E$  combined with an adjustment of  $f_s$ . One could also improve the evaluation of the profiles in the cooling layer and adaptation zone, and extend the accuracy of the solution to weaker shocks, by iterating the profile of the mean intensity.

Our goal in the present work has been to develop the simplest possible model that captures the essential behavior of OTR shocks. Alternatively, given sufficient computational resources and expertise, one could develop calculations that solve the radiative transfer calculations to high numerical accuracy and also iterated to find a self-consistent shock structure. This might, for example, involve the use of a variable Eddington factor [such that both  $f_E$  and  $J_R$  remain within the derivative of Eq. (11) above]. Calculations using variable Eddington factors are discussed, with references to the historical literature, on pp. 263–265 in the book by Castor.<sup>24</sup> Such calculations would complement the work reported here.

The self-consistent calculation presented here, made possible by the realization that the mean intensity is essentially constant throughout an optically thin cooling layer for strong OTR shocks, allows rapid evaluation of the structure of radiative shocks in optically thick media. This should prove useful for experiment design and data analysis, while the solutions presented here provide a test case for simulations. In applications, one implication of the present work is that the observation of a diffusive structure in a precursor, for example as a shock emerges into view at the surface of a star, has no particular implications regarding the downstream conditions and cannot directly be used to infer the downstream temperature.

## ACKNOWLEDGMENTS

John Castor has produced some (as yet unpublished) work in the direction of developing a complete solution of the radiative transfer aspects of OTR shocks. The present paper has benefited from discussions with him of his work. The author acknowledges useful discussions of this subject with Dmitri Ryutov, Serge Bouquet, and John Edwards.

Financial support was provided by the National Nuclear Security Administration under the Stewardship Science Academic Alliances program through DOE Research Grant No. DE-FG52-03NA00064.

## APPENDIX

Here we add some detailed remarks regarding the work of Sincell, Gehmeyer, and Mihalas,<sup>21</sup> referred to here as SGM. These remarks are in no respect intended to diminish the value of the advances in numerical technique that led to the subject work. They are, however, a call for careful attention to fundamental physics when validating complex simulation codes. They are in part a response to comments of more than one past referee to the effect that OTR shocks are on the whole well understood and are accurately described in the literature. It is worth noting that the discussion in the literature prior to SGM, including that in the key historical books is more oriented toward the challenges of handling the radiation transport than toward a clear description of the underlying physics of such shocks.

SGM undertake the simulation of radiative shocks in the “subcritical” and “supercritical” regimes. Our remarks here pertain to the second case, in which SGM simulates a shock wave having  $Q \sim 10^5$  with  $\gamma = 5/3$ . They include a section on analytic theory in which they present [as their Eq. (11)] equations that are identically equivalent to the relations given above as Eqs. (3), (4), and (6). They then proceed to follow Zel’dovich and Raizer by expanding these relations to first order in the final inverse compression (labeled as  $\eta_1$  in SGM) and to compare their simulation results to the resulting approximate expressions. They show (in their Figs. 5, 6, and 10) that the results of their simulations do not reproduce the curves generated by these expressions. They then make qualitative arguments regarding the effects of higher order (i.e., second-order) terms in  $\eta_1$ .

This aspect of the presentation in SGM deserves discussion. The fundamental equations [Eq. (11) in SGM, and Eqs. (3), (4), and (6) above] represent the conservation of mass, momentum, and energy in this system. No aspect of radiation transport can invalidate these equations. Moreover, these equations apply on a point-by-point basis throughout the system (including across any transitions whether instantaneous or not). This point is discussed in much more depth in pp. 301–309 in Drake.<sup>1</sup> Any simulation whose results do not lie on the exact curves generated by these equations does not conserve mass, momentum, and energy. The present author would urge future authors of simulation results to do the trivial amount of work necessary to generate such exact curves and to compare their results to them.

In addition, SGM do not correctly analyze other aspects of their results. First, they find a zone in which the sign of the radiation flux reverses, as shown for example in their Fig. 7. This they interpret as a consequence of temperature gradients in the cooling layer, yet they fail to realize that this fundamentally represents a violation of energy conservation and thus cannot be correct. Second, in discussing the cooling layer, they state that “the area under the optically thin temperature spike must be conserved” in discussing the role of artificial viscous heating. This is not correct. What must be conserved is the generation of radiative flux in the cooling layer, as one can determine by contemplating the implications of Eq. (6) above or alternatively the energy balance discussed in Sec. IV above and on pp. 324–326 in Drake.<sup>1</sup>

Third, they argue based on their simulations that the approximate equation for the maximum postdensity-jump temperature [their Eq. (23)] is more accurate than the “exact” value  $[(3-\gamma)T_f]$  correctly given by Razier<sup>30</sup> without derivation. They should have understood that the exact value is a physical limit based on the conservation laws, derived it themselves, and explored why their code did not produce it.

This section closes by re-emphasizing the value of the development of advanced radiation hydrodynamic methods and of their application to radiative shocks, to which SGM made an important contribution. Above and beyond the numerics, it remains crucial to carry through with sound physical thinking and comparison where possible with exact physics.

<sup>1</sup>R. P. Drake, *High Energy Density Physics: Fundamentals, Inertial Fusion and Experimental Astrophysics* (Springer Verlag, Berlin, 2006).

<sup>2</sup>S. Bouquet, C. Stehlé, M. Koenig *et al.*, Phys. Rev. Lett. **92**, 225001-1 (2004).

<sup>3</sup>Y. B. Zel’dovich and Y. P. Razier, *Physics of Shock Waves and High-Temperature Hydrodynamic Phenomena* (Dover, New York, 2000).

<sup>4</sup>M. J. Edwards, A. J. MacKinnon, J. Zweiback *et al.*, Phys. Rev. Lett. **87**, 085004-1 (2001).

<sup>5</sup>D. Mihalas and B. Weibel-Mihalas, *Foundations of Radiation Hydrodynamics* (Dover, New York, 1984).

<sup>6</sup>S. K. Chakrabarti and L. G. Titarchuk, Astrophys. J. **455**, 623 (1995).

<sup>7</sup>R. Sivron, D. Caditz, and S. Tsuruta, Astrophys. J. **469**, 542 (1996).

<sup>8</sup>A. V. Farnsworth and J. H. Clarke, Phys. Fluids **14**, 1352 (1971).

<sup>9</sup>Yu. A. Fadeyev and D. Gillet, Ann. N.Y. Acad. Sci. **333**, 687 (1998).

<sup>10</sup>M. S. Bessell, M. Scholz, and P. R. Wood, Ann. N.Y. Acad. Sci. **307**, 481 (1996).

<sup>11</sup>L. Boireau, C. Clique, and S. Bouquet, Radiative Shocks in Low-Pressure Gases, in Proceedings of the Inertial Fusion Science and Applications, Monterey, CA, 2003, edited by B. A. Hammel, D. D. Meyerhofer, J.

Meyer-ter-Vehn, and H. Azechi (American Nuclear Society, New York, 2004), p. 966.

<sup>12</sup>L. Boireau, Ph.D. thesis, University de Paris VI, 2005.

<sup>13</sup>J. C. Bozier, G. Thiell, J. P. Le-Breton *et al.*, Phys. Rev. Lett. **57**, 1304 (1986).

<sup>14</sup>A. D. Edens, T. Ditmire, J. F. Hansen *et al.*, Phys. Plasmas **11**, 4968 (2004).

<sup>15</sup>P. A. Keiter, R. P. Drake, T. S. Perry *et al.*, Phys. Rev. Lett. **89**, 165003-1 (2002).

<sup>16</sup>M. Koenig, A. Benuzzi-Mounaix, N. Grandjouan *et al.*, in *Proceedings of Shock Compression of Condensed Matter*, Atlanta, Georgia, 2001, edited by M. D. Furnish, Y. Horie, and N. N. Thadhani (American Institute of Physics, New York, 2002), Vol. 620, Part 2, pp. 1367.

<sup>17</sup>A. B. Reighard, R. P. Drake, K. K. Danneberg *et al.*, *Collapsing Radiative Shocks in Xenon Gas on the Omega Laser*, in Proceedings of the Inertial Fusion and Science Applications, Monterey CA, 2003, edited by B. A. Hammel, D. D. Meyerhofer, J. Meyer-ter-Vehn, and H. Azechi (American Nuclear Society, New York, 2004), p. 950.

<sup>18</sup>A. B. Reighard, R. P. Drake, K. K. Danneberg *et al.*, Phys. Plasmas **13**, 082901 (2006).

<sup>19</sup>T. J. Nash, M. S. Derzon, G. A. Chandler *et al.*, Phys. Plasmas **6**, 2023 (1999).

<sup>20</sup>S. G. Glendinning, Lawrence Livermore National Laboratory (private communication, 2006).

<sup>21</sup>M. W. Sincell, M. Gehmeyr, and D. Mihalas, Shock Waves **9**, 391 (1999).

<sup>22</sup>N. J. Turner and J. M. Stone, Astrophys. J., Suppl. Ser. **135**, 95 (2001).

<sup>23</sup>S. C. Traugott, Phys. Fluids **8**, 834 (1965).

<sup>24</sup>J. Castor, *Radiation Hydrodynamics* (Cambridge University Press, Cambridge, 2004).

<sup>25</sup>K-H. A. Winkler, M. L. Norman, and D. Mihalas, in *Multiple Time Scales*, edited by J. U. Brackbill and B. I. Cohen (Academic, New York, 1985), p. 145.

<sup>26</sup>D. D. Ryutov, R. P. Drake, J. Kane *et al.*, Astrophys. J. **518**, 821 (1999).

<sup>27</sup>S. Bouquet, R. Teyssier, and J. P. Chieze, Astrophys. J., Suppl. Ser. **127**, 245 (2000).

<sup>28</sup>M. A. Heaslet and B. S. Baldwin, Phys. Fluids **6**, 781 (1963).

<sup>29</sup>A. B. Fokin, G. Massacrier, and D. Gillet, Ann. N.Y. Acad. Sci. **420**, 1047 (2004).

<sup>30</sup>Iu. P. Raizer, Sov. Phys. JETP **5**, 1242 (1957).